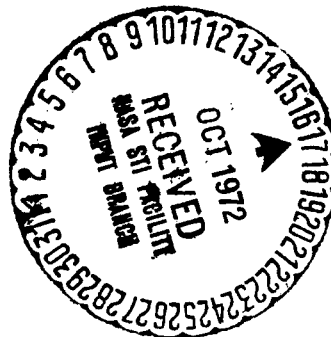


WIND TUNNEL CORRECTIONS FOR MEASUREMENTS OF TWO-DIMENSIONAL  
PROFILES IN THE TRANSONIC WIND TUNNEL OF THE  
AERODYNAMIC TESTING FACILITY GÖTTINGEN

P. Mackrodt

(NASA-TT-F-14316) WIND TUNNEL CORRECTIONS  
FOR MEASUREMENTS OF TWO-DIMENSIONAL  
PROFILES IN THE TRANSONIC WIND TUNNEL OF  
THE P. Mackrodt (Scientific Translation  
Service) Jun. 1972 16 p CSCL 14B G3/11 43332  
N72-32264 Unclass

Translation of: "Windkanalkorrekturen bei  
Messungen an zweidimensionalen Profilen im  
Transsonischen Windkanal der Aerodynamischen  
Versuchsanstalt Göttingen," Zeitschrift fuer  
Flugwissenschaften, Vol. 19, Nov. 1971,  
pp. 449-454.



WIND TUNNEL CORRECTIONS FOR MEASUREMENTS OF TWO-DIMENSIONAL  
PROFILES IN THE TRANSONIC WIND TUNNEL OF THE  
AERODYNAMIC TESTING FACILITY GÖTTINGEN

Paul-Armin Mackrodt \*

ABSTRACT. Pressure distribution measurements on an airfoil at high subsonic speed were carried out in the transonic wind tunnel of the AVA Göttingen of the DFVLR. The normal force coefficients obtained from these pressure distributions were corrected for wind tunnel interferences and compared with results of theoretical calculations. To this end the wind-tunnel wall corrections for two-dimensional flow given in the literature were adapted to the special case of the transonic wind tunnel of the AVA.

1. Notation

/449\*\*

In the present work we will use the notation according to the Norm LN 9300. Therefore we will only specify notations which are not defined in LN 9300 or whose numerical magnitude is required for understanding the text.

1.1. Geometrical Quantities (Figures 1, 2, 3)

- b - Span of the model ( $b = 1 \text{ m}$ )
- F - Reference area ( $= b\bar{z}$ ) ( $F = 0.2 \text{ m}^2$ )
- $F_p$  - Cross section area of the profile ( $F_p = 34.3 \text{ cm}^2$ )
- $F_s$  - Cross section area of the test section ( $F_s = 1 \text{ m}^2$ )

---

\* Aerodynamic Experimental Test Facility, Göttingen of the German Research and Test Facility for Aerodynamics and Space Flight (DFVLR).

\*\* Numbers in the margin indicate pagination in the original foreign text.

- H - Tunnel height ( $H = 1 \text{ m}$ )
- l - Profile chord ( $l = 200 \text{ m}$ )
- x - Coordinate in the profile plane  $x = 0$  in the profile leading edge
- $x_{25}$  - Distance of the moment reference axis from the profile leading edge ( $=l/4$ )
- z - Coordinate perpendicular to x and to the span direction,  $z = 0$  along the profile chord

### 1.2. Flow Quantities

- $c_p$  - Pressure coefficient [ $= (p - p_\infty)/q_\infty$ ]
- p - Static pressure
- Re - Reynolds number ( $= \rho U l / \mu$ )
- u - Additional velocity induced by the blockage
- U - Flow velocity
- $\delta_0, \delta_1$  - Correction factors for the influence of the wall perforation on the induced stream deflection
- $\epsilon$  - Relative additional velocity ( $= u/U$ ); Equation (8) to (11)
- $\kappa$  - Adiabatic exponent ( $\kappa = 1.4$  for air)
- $\mu$  - Dynamic viscosity of air
- $\Omega$  - Ratio of the additional velocities u for solid and perforated channel walls; Equations (12) and (13)

### 1.3. Subscripts

- M - Quantities depending on the model
- T - Quantities depending on the wake
- $\infty$  - Quantities of the undisturbed flow

## 2. Introduction

As a rule wind tunnels for the transonic velocity range have test sections with slotted walls. They can also be perforated, as for example in the transonic wind tunnel of the AVA. Part of the air flowing through is

sucked away through the perforation holes, so that the boundary layer at the wall has uniform thickness over the entire measurement test section length and so that the Mach number remains constant (see for example B. B. H. Goethert [1] as well as Section 3). Because of this suction the flow around a profile located in such a test section is not two dimensional if the ratio of the profile chord to the channel width (= span) is too large. This deviation from the two-dimensional flow then will certainly become smaller if symmetrical parts of the channel sidewalls are made impermeable with respect to the profile model. In other words, they are made in the form of end plates. In order to test the reliability of results of profile measurements using such an arrangement, we carried out experiments in the transonic wind tunnel of the AVA using a profile with the ratio  $l/H = 0.2$ . Pressure distribution measurements at  $Ma_{\infty} = 0.72$  were carried out and the measurement results which were corrected for the finite jet dimension effects were compared with the results of theoretical calculations. For this purpose it was necessary to determine the wind tunnel corrections for two-dimensional flows from the literature. These were then recalculated for the special conditions in the transonic wind tunnel of the AVA.

### 3. Experimental Measurement and Arrangement

The measurements were performed in the continuously operating transonic wind tunnel of the AVA. The test section of the tunnel has perforated walls and the jet cross section is  $F_s = 1 \text{ m} \times 1 \text{ m}$ . Detailed descriptions of the tunnel are found in H. Ludwig, W. Lorenz-Meyer and W. Schneider [2] as well as in Th. Hottner and W. Lorenz-Meyer [3].

The pressure distribution measurements were carried out on a NACA 64 A 213 profile which was made available by the firm Dornier GmbH (see [4]). The model made out of one piece of steel has a chord of  $l = 200 \text{ mm}$  and a thickness ratio of 13%. The profile coordinates are given in Table 1. Forty-eight pressure holes having a diameter of  $0.5 \text{ mm}$  are arranged one after the other around the central circumference of the profile. Thirty of these

TABLE 1. COORDINATES OF THE PROFILE R 1

x [mm]	Upper Surface	Lower Surface
	z [mm]	z [mm]
0,0	0,000	0,000
10,0	6,046	- 6,048
20,0	8,332	- 8,312
30,0	9,930	- 9,938
40,0	11,097	- 11,160
50,0	11,944	- 12,058
60,0	12,518	- 12,670
70,0	12,828	- 13,022
80,0	12,846	- 13,100
90,0	12,514	- 12,854
100,0	11,912	- 12,336
110,0	11,104	- 11,572
120,0	10,138	- 10,604
130,0	9,054	- 9,458
140,0	7,866	- 8,194
150,0	6,592	- 6,864
160,0	5,284	- 5,508
170,0	3,976	- 4,154
180,0	2,668	- 2,798
190,0	1,362	- 1,424
200,0	0,054	- 0,054

are on the upper surface and 17 on the lower surface, and one on the profile nose. Figure 1 shows their positions around the profile.

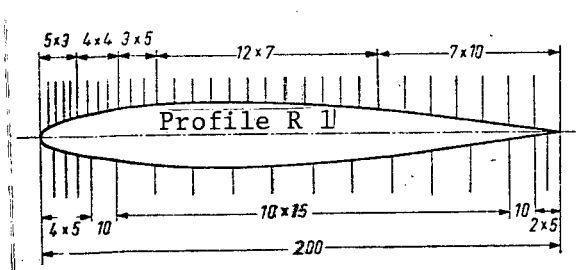


Figure 1. Profile R 1 with position of the pressure holes.

The model is held at the ends by nonperforated circular plates having a diameter of 450 mm which form a plane with the test section wall. These plates are supported by the holding devices which transfer forces applied to the model to the tunnel walls. Figure 2 shows the

basic construction. The holding devices are mounted on ball bearings in the wind tunnel test section walls so they can rotate. Thus the model can rotate about its

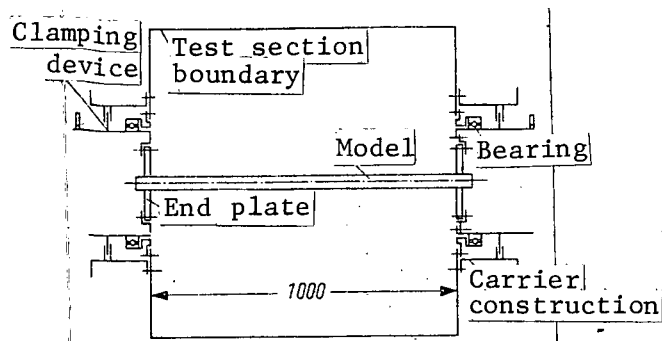


Figure 2. Arrangement of the profile in the test section of the transonic wind tunnel.

transverse axis and therefore the angle of attack can change. During the measurements the model is prevented from moving by means of clamping devices.

Since the holding devices and the ball bearings are not perforated, the model ends are surrounded by nonperforated end plates having an approximate diameter of about 550 mm (= 2.75 l) in the otherwise perforated

tunnel wall (Figure 3). According to the experiments made so far (see for example F. W. Riegels [5]), it can be assumed that the two-dimensional flow has been sufficiently well established.

#### 4. Execution of the Measurements and Presentation of the Results

The pressure distribution measurements were carried out at the free-stream Mach number  $Ma_\infty = 0.72$  for the angle of attack range  $0^\circ \leq \alpha \leq 8^\circ$ . The Reynolds number (based on the wing chord) was  $Re_\infty = 2.3 \cdot 10^6$ . The results of the pressure distribution measurements were reported in detail in [16]. We will not repeat them here.

The normal force coefficients are determined from the pressure distributions by integration. They are shown in Figure 4 in the form  $c_z(\alpha)$ .

#### 5. Wind Tunnel Corrections

Based on the construction of the transonic wind tunnel of the AVA, the wind tunnel corrections for three-dimensional models are always very small, as W. Lorenz-Meyer [6] showed. However, this is not true for two-dimensional

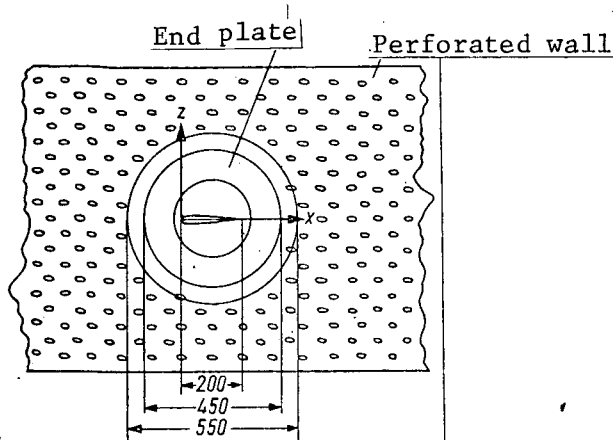


Figure 3. End plates in the perforated wall of the measurement test section of the transonic wind tunnel.

models. Therefore in the following we will give the downwash corrections and the blockage corrections according to H. C. Garner et al. [7]. We also give the stagnation pressure gradient correction. Because of the relatively large end plates (see Section 3), we can use the corrections for the strictly two-dimensional flow in the case under discussion here.

All corrections are applied by adding the correction quantity to the uncorrected measured value:

$$\overline{\alpha_{\text{corr}}} = \alpha + \Delta\alpha. \quad (1)$$

### 5.1. Stream Deflection Corrections

In the calculation of the stream deflection corrections in [7], the two-dimensional wing is represented by a single infinitely long vortex filament

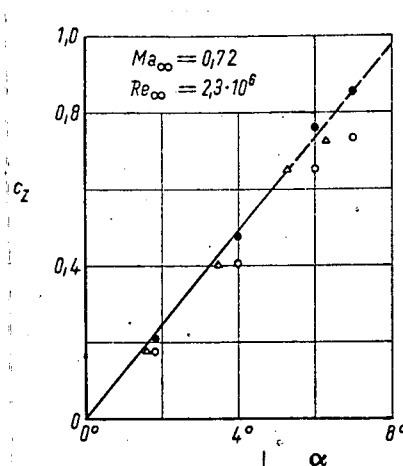


Figure 4. Corrected and uncorrected normal force coefficients as a function of the angle of attack  $\alpha$  for  $Ma_\infty = 0.72$  and  $Re_\infty = 2.3 \cdot 10^6$  compared with the theoretical results.

- - uncorrected values
- - corrected according to Equations (7) and (17), respectively
- △ - corrected according to Equations (2) and (3)
- Theory according to calculations of the firm Dornier GmbH.

which runs in the span direction. The downwash induced by this vortex filament and the infinite number of mirror images (produced by reflection at the stream boundaries) deflects the jet at the location of the (finite) model and therefore requires corrections in the angle as well as in the coefficients. According to [7] these corrections are given by:

$$\Delta\alpha = c_z \frac{l}{H} \delta_0 + \left( \frac{l}{H} \right)^2 \frac{\delta_1}{\sqrt{1 - Ma_\infty^2}} \left( \frac{1}{4} c_z + c_M \right), \quad (2)$$

$$\Delta c_z = - \frac{\pi}{2} \left( \frac{l}{H} \right)^2 \frac{c_z}{1 - Ma_\infty^2} \delta_1, \quad (3)$$

$$\Delta c_M = \frac{\pi}{8} \left( \frac{l}{H} \right)^2 \frac{c_z}{1 - Ma_\infty^2} \delta_1. \quad (4)$$

The angle of attack correction (2) and the curvature correction (3) can be summarized in a total correction of the normal force coefficient (stream deflection correction) as follows:

$$\Delta c_z = - \frac{2\pi}{\sqrt{1 - Ma_\infty^2}} \Delta\alpha - \frac{\pi}{2} \left( \frac{l}{H} \right)^2 \frac{c_z}{1 - Ma_\infty^2} \delta_1. \quad (5)$$

After substitution of  $\Delta\alpha$  and assuming that

$$c_M \ll c_z \quad (6)$$

which is permissible here, we finally obtain the following for the stream deflection correction:

$$\left\{ - \frac{\Delta c_z}{c_z} = 2\pi \frac{l}{H} \frac{\delta_0}{\sqrt{1 - Ma_\infty^2}} + \right. \quad (7)$$

$$\left. + \pi \left( \frac{l}{H} \right)^2 \frac{\delta_1}{1 - Ma_\infty^2} \right.$$

The factors  $\delta_0$  and  $\delta_1$  represent the influence of the type of jet boundaries. For the free jet we have  $\delta_0 = -1/4$  and  $\delta_1 = \pi/12$ . For the closed test section we have  $\delta_0 = 0$  and  $\delta_1 = \pi/24$ . However, we would like to point out that Equation (7) does not transform into the corrections given by W. Hantzsche and H. Wendt [8], because in [8] the model is not represented by a (single) vortex



filament when the corrections were calculated. Instead it is represented by a vortex sheet covering a flat plate having an infinite span with the chord  $l$ . The quantities  $\delta_0$  and  $\delta_1$  were determined for perforated walls according to H. C. Garner et al. [7] using the specific data for the transonic wind tunnel of the AVA given by W. Lorenz-Meyer [6]. In Figure 5 they are plotted as a function of the freestream Mach number. Using these values, the downwash corrections for the coefficients  $c_z$  and  $c_M$  were calculated according to equations (3), (4) and (7). Figure 6 shows them calculated according to Equations (3) and (4) and plotted against the freestream Mach number. Figure 7 shows them calculated according to Equations (7) and plotted against the freestream Mach number. The correction for the angle of attack, Equation (2), was plotted for the design Mach number  $Ma_\infty = 0.72$  and is plotted in Figure 8 as a function of the (uncorrected) normal force coefficient  $c_z$ .

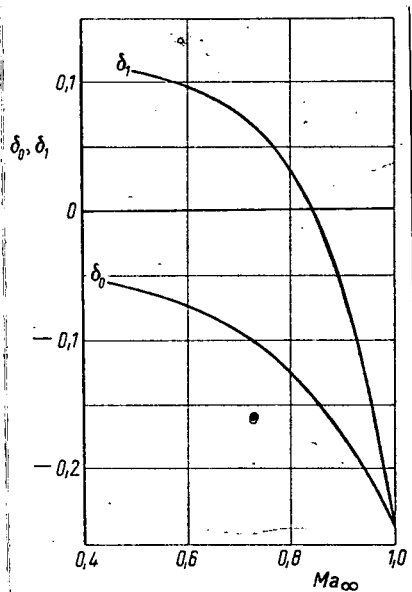


Figure 5. Wall influence parameters for the downwash corrections.

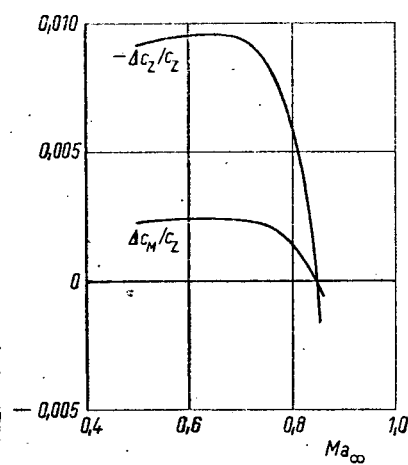


Figure 6. Stream deflection corrections according to Equations (3) and (4) as a function of the freestream Mach number.

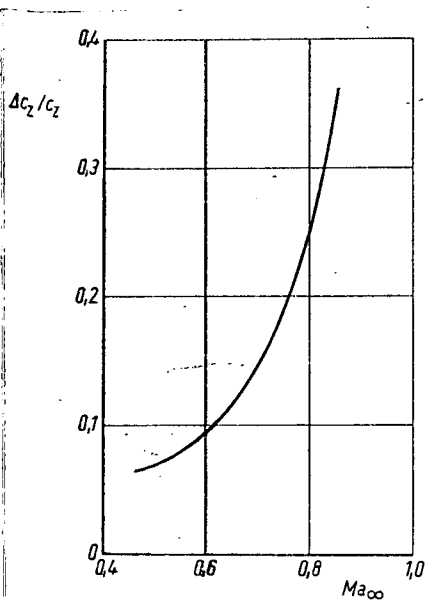


Figure 7. Stream deflection corrections according to Equation (7) as a function of the freestream Mach number.

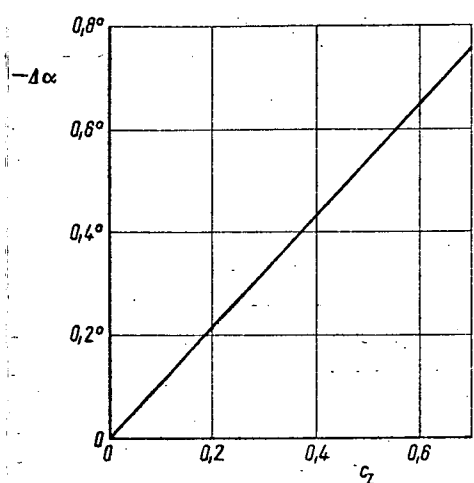


Figure 8. Angle of attack correction according to Equation (2) for  $Ma_\infty = 0.72$  as a function of the normal force coefficient.

## 5.2. Blockage Corrections

The following equations were given by H. C. Garner et al. [7] for the blockage corrections:

$$\frac{\Delta Ma}{Ma} = \left(1 + \frac{\kappa - 1}{2} Ma_\infty^2\right) (\varepsilon_M + \varepsilon_T), \quad (8)$$

$$\Delta c_p = [2 - (2 - Ma_\infty^2) c_p] (\varepsilon_M + \varepsilon_T), \quad (9)$$

$$\left\{ \begin{array}{l} \frac{\Delta c_i}{c_i} = -(2 - Ma_\infty^2) (\varepsilon_M + \varepsilon_T) \\ (i = A, M, W, X, Z) \end{array} \right. \quad (10)$$

If in the correction for the drag coefficient  $c_w$  we also include the correction due to the wake blockage pressure gradient, we have

$$\left\{ \begin{aligned} \frac{\Delta c_W}{c_W} = - \{ [1 + (\kappa - 1) Ma_\infty^2] \varepsilon_M + \\ + (2 - Ma_\infty^2) (\varepsilon_M + \varepsilon_T) \} \end{aligned} \right. \quad (11)$$

For  $\varepsilon_M$  and  $\varepsilon_T$  and the two-dimensional case we have the following, according to [7]:

$$\varepsilon_M = \frac{\pi}{6} \frac{F_P}{H^2} \frac{\Omega_M}{(1 - Ma_\infty^2)^{3/2}} \quad (12)$$

$$\varepsilon_T = \frac{c_W}{4} \frac{l}{H} \frac{\Omega_T}{1 - Ma_\infty^2} \quad (13)$$

The parameters  $\Omega_M$  and  $\Omega_T$  specify the influence of the type of jet boundaries. They are plotted in Figure 9 as a function of the freestream Mach number and were recalculated according to H. G. Garner et al. [7] and using the specific values for the transonic wind tunnel of the AVA given by W. Lorenz-Meyer [6].

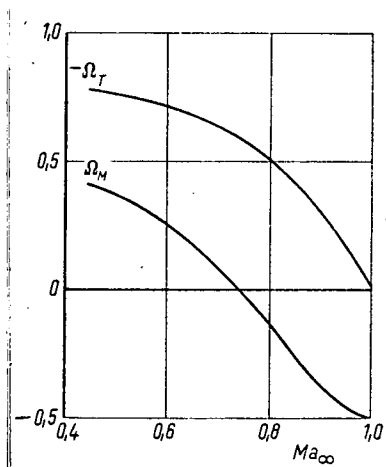


Figure 9. Wall influence parameter for the blockage corrections.

For the free jet, we have  $\Omega_M = -1/2$  and  $\Omega_T = 0$ . For the tunnel closed on all sides we have  $\Omega_M = \Omega_T = 1$ . After substituting these values in (12) and (13) and also substituting  $\varepsilon_M$  and  $\varepsilon_T$  in Equations (8) to (11), we can see that they do not transform into the equations given by H. Ludwig [9] for these special cases. The reason for this is that in [7], H. Ludwig [10] did not consider the fact that in compressible flows the

wake blockage increases with  $1 + (\kappa - 1) Ma_\infty^2$ , because in the wake there is a density reduction in addition to a velocity loss. If we consider this effect, then Equations (8), (9) and (10) become:

$$\left\{ \begin{array}{l} \frac{\Delta Ma}{Ma} = \left(1 + \frac{\kappa - 1}{2} Ma_{\infty}^2\right) \times \\ \times \{ \varepsilon_M + \varepsilon_T [1 + (\kappa - 1) Ma_{\infty}^2] \}, \end{array} \right. \quad (14)$$

$$\left\{ \begin{array}{l} \Delta c_p = [2 - (2 - Ma_{\infty}^2) c_p] \times \\ \times \{ \varepsilon_M + \varepsilon_T [1 + (\kappa - 1) Ma_{\infty}^2] \}, \end{array} \right. \quad (15)$$

$$\left\{ \begin{array}{l} \frac{\Delta c_i}{c_i} = -(2 - Ma_{\infty}^2) \times \\ \times \{ \varepsilon_M + \varepsilon_T [1 + (\kappa - 1) Ma_{\infty}^2] \}. \end{array} \right. \quad (16)$$

The Equation (11) for  $\Delta c_W / c_W$  remains unchanged. We only have to substitute the value of  $\Delta c_i / c_i$  calculated according to Equation (16).

In order to calculate the blockage corrections we took over the required values for  $c_W$  from the measurements described in [4] for the Mach number range of interest here ( $0.5 \leq Ma_{\infty} \leq 0.85$ ) and for a constant angle of attack ( $\alpha = 1.8^\circ$ ). Using these values, we calculated the blockage corrections according to Equations (8), (10) and (11) as well as Equations (14) and (16). Both are plotted in Figure 10 as a function of the freestream Mach number.

## 6. Comparison of the Measurement Results with the Results of Theory

Pressure distributions and normal force coefficients were calculated by the firm Dornier GmbH for the investigated wing profile using the method of C. S. Sinnott [11]. It was programmed by H. Körner [12]. The calculation was first performed for invicid flow and the calculated normal force increases or angles of attack, respectively, were corrected for finite Reynolds numbers ( $Re_{\infty} = 2.3 \cdot 10^6$  here) using methods described in [13] and [14]. The method given in [13] assumes a turbulent boundary layer beginning at the profile nose. In addition, [14] gives a correction method for the case where the boundary layer becomes turbulent only after 50% of the profile chord. For the profile investigated here, the correction factors for these two cases differ by only 2.3% according to [14]. According to the same reference,

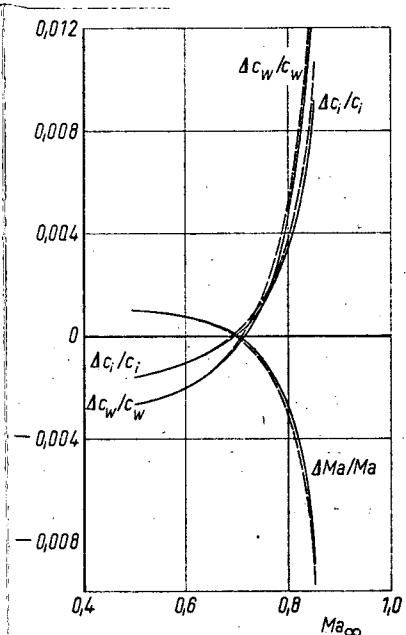


Figure 10. Blockage corrections

- according to Equations (8), (10) and (11);  
 - - - according to Equations (14) and (16)

H. Schlichting [15]). In the case of the profile investigated here, this occurs at about 38% of the wing chord (Figure 1, Table 1) for the angle of attack  $\alpha = 0^\circ$ , i.e., we can count on a boundary layer transition in the range  $x/l \approx 0.4$ .

Figure 4 shows the uncorrected measurement values together with the theoretical results as well as the corrected measurement results. The measurement values were corrected according to Equations (2) and (3) as well as Equation (7). As can be seen from Figure 7, at  $Ma_\infty = 0.72$  the stream deflection correction becomes

$$\Delta c_z/c_z = 0.164 \quad (17)$$

the factors have an error of  $\pm 5\%$ . This means that within the achievable accuracy, the corrected value calculated assuming a turbulent boundary layer beginning at the profile nose will still be valid if the boundary layer changes over anywhere between  $x/l = 0$  and  $x/l = 0.5$ .

In order to allow a comparison of these theoretical results with those of the measurements carried out here, we must be sure that the boundary layer and the investigated profile model will carry out a transition in the range  $x/l \leq 0.5$  without any artificial means. On clean profiles, the boundary layer transition occurs just behind the pressure minimum (see for example

From Figure 4 it can be seen that the corrected measurement values agree extremely well with the theoretical results.

## 7. Summary

Pressure distribution measurements on a profile having nonperforated end plates were carried out at  $Ma_\infty = 0.72$  in the transonic wind tunnel of the AVA in order to establish the reliability of the measurements on profiles placed in the test section of wind tunnels having perforated walls. In order to compare the measurements with theory, the wind tunnel corrections for two-dimensional flows were determined from the literature for the special case of the transonic wind tunnel of the AVA. It was found that the blockage corrections are smaller than 1% within the Mach number range considered ( $0.5 \leq MA \leq 0.85$ ). The stream deflection corrections are significantly larger and amount to  $\Delta c_z / c_z = 0.07$  for  $Ma_\infty = 0.5$  and  $\Delta c_z / c_z = 0.36$  for  $Ma_\infty = 0.85$ .

A comparison of the measured values corrected in this way with the theoretical results shows excellent agreement. Therefore it has been shown that reliable measurements can be made on profiles having considerable chord distances in wind tunnels which have perforated test section walls and which operate in the high subsonic range. This is done by installing impermeable end plates having a diameter of about three profile chords. However, the chord of the profile models cannot be larger than 20% of the width of the test section because of the relatively large stream deflection corrections for measurements in the range  $Ma_\infty \leq 0.75$ . If measurements are carried out at large freestream Mach numbers, it cannot exceed 15% of this width.

## REFERENCES

1. Goethert, B. H. Transonic Wind Tunnel Testing. AGARDograph, Vol. 49, 1961.
2. Ludwig, H., W. Lorenz-Meyer, and W. Schneider. Der Transsonische Windkanal der Aerodynamischen Versuchsanstalt Göttingen (Transonic Wind Tunnel of the Aerodynamic Experimental Installation Göttingen). 1966 yearbook of WGLR, pp. 145-155.
3. Hottner, Th., and W. Lorenz-Meyer. Der Transsonische Windkanal der AVA Göttingen (Transonic Wind Tunnel of the Aerodynamic Experimental Installation Göttingen), Second Development Stage. 1968 yearbook of the DGLR, pp. 235-244.
4. Mackrodt, P.-A. and H. Grauer-Carstensen. Druckverteilungsmessungen an drei Profilen im Transsonischen Windkanal der AVA (Pressure Distribution Measurements and Three Profiles in the Transonic Wind Tunnel of the AVA). AVA Report 66 A 63, 1967.
5. Riegels, F. W. Aerodynamische Profile. 1 Auflage (Aerodynamic Profile, First Stage). R. Oldenbourg, Munich, 1958.
6. Lorenz-Meyer, W. Tunnel Corrections for the Transonic Wind Tunnel of the Aerodynamic Experimental Installation Göttingen for Measurements on Three Dimensional Models. Z. Flugwiss., Vol. 19, 1971, pp. 454-461.
7. Garner, H. C., E. W. E. Rogers, W. E. A. Acum and E. C. Maskell. Subsonic Wind Tunnel Wall Corrections. AGARDograph, Vol. 109, 1966.
8. Hantzsche, W. and H. Wendt. Windkanalkorrekturen bei kompressiblen Strömungen (Wind Tunnel Corrections for Compressible Flows). 1941 yearbook of German aeronautics, pp. I 678 - I 683.
9. Ludwig, H. Windkanalkorrekturen bei kompressibler Strömung (Wind Tunnel Corrections for Compressible Flow). Göttingen Monograph, Vol. D<sub>3</sub> 4.2, 1947.
10. Ludwig, H. Widerstandskorrektur in Hochgeschwindigkeitskanälen (Drag Correction in High Velocity Wind Tunnels). AVA Report 44 H 08, 1944 and Luftfahrtforschung ZWB, FB 1955, 1944. English translation: NACA TM 1163, 1946.
11. Sinnott, C. S. Theoretical Prediction of the Transonic Characteristics of Airfoils. J. Aerospace Sci., Vol. 29, 1962, p. 275.

12. Körner, H. Berechnung der Druckverteilungen in den charakteristischen Schnitten eines Pfeilflügels mit Hilfe eines FORTRAN-Rechenprogramms (Calculation of the Pressure Distributions in Characteristic Cross Sections of a Swept Back Wing Using a Fortran Computer Program). Institute for Aerodynamics for the DFL, Braunschweig, Report 67 R 06, 1967.
13. Royal Aeronautical Society: Transonic Data Memorandum 6407, 1964.
14. Royal Aeronautical Society: Aerodynamics Data Sheet Wings 01.01.05, 1955.
15. Schlichting, H. Grenzschicht-Theorie, 5. Aufl. (Boundary Layer Theory, Fifth Ed.). Verlag G. Braun, Karlsruhe, 1965, p. 428.
16. Mackrodt, P.-A. Wandeinfluss und Windkanalkorrekturen bei Druckverteilungsmessungen an Profilen im Transsonischen Windkanal der AVA (Wall Influence and Wind Tunnel Corrections for Pressure Distribution Measurements on Profiles in the Transonic Wind Tunnel of the AVA). AVA Report 69 A 01, 1969.

Translated for National Aeronautics and Space Administration under contract No. NASw 2035, by SCITRAN, P. O. Box 5456, Santa Barbara, California, 93108.